

Ref:

Date: 18 February 2003

MEMORANDUM

From : Eugene Chudakov, JLab
To : ...
Subject : Electromagnetic Impact of CEBAF Beam on Hydrogen Trap

EXPECTED IMPACT OF CEBAF BEAM ON HYDROGEN TRAP

Abstract

A magnetic ultra-cold trap of fully polarized atomic hydrogen is being considered for using as a target for Møller polarimetry at CEBAF, at beam currents up to 100 μA . This note addresses possible problems caused by the CEBAF beam impact on such a target. The beam current generates an electromagnetic RF radiation which may cause a target depolarization inducing spin flips. Also, a part of the radiation may be absorbed in the cell pipe, heating it. The beam also heats up the gas by ionization.

1 Introduction

Atomic hydrogen stored in an ultra-cold magnetic trap, can provide a 100%-polarized target for electron Møller polarimetry, as well as a $\sim 80\%$ polarized proton target for scattering at angles close to zero. The technique of such traps is well developed (see, for example [1]) and it has been applied to accelerator experiments. However, such a trap has not been used as a target, with a high current beam circulating through it. Such a beam creates a powerful electromagnetic radiation (RF), as well as ionization of the gas. This may cause several problems:

- Depolarization of hydrogen by the RF radiation;
- Heating of the cell by absorption of the RF radiation;
- Depolarization of hydrogen caused by ionization heating;
- Heating up the cell by ionization.

This note contains an estimate of these effects.

2 Parameters of the Beam and the Trap

2.1 Beam

The beam parameters considered are as follows:

- $\sigma_{Bt} = \tau = 0.5$ ps - bunch time width (RMS) in LAB frame

- σ_{Br} = 100 μm - bunch radial width (RMS) in LAB frame
- \mathcal{F} = 497 MHz - bunch repetition rate
- $\gamma \sim 10^4$ - beam γ -factor
- \mathcal{I}_b = 100 μA - average beam current

Gaussian shapes are assumed for both the longitudinal and transverse beam profiles.

2.2 Hydrogen Trap

The atomic hydrogen trap consists of a copper pipe being a part of the dilution refrigerator, kept at 300 mK.

The parameters of the copper pipe are:

- L = 0.4 m - pipe length
- r_0 = 0.02 m - pipe diameter
- σ = 10^{11} (ohm·m)⁻¹ - copper conductance at 300 mK
- $T \sim 0.3$ K - the temperature
- $\frac{dN}{dV} \sim 3 \cdot 10^{15}$ atoms/cm² - the gas density

2.3 Other Parameters and Constants Used

Some derived parameters are used:

- $q = \mathcal{I}_b/\mathcal{F} = 0.2$ pC - bunch charge
- $\sigma_{Bz} = \sigma_{Bt} \cdot c = 150\mu\text{m}$ - bunch longitudinal width (RMS) in LAB frame
- $\rho(z, r) = q/(\sqrt{2\pi}\sigma_{Bz}) \cdot \exp(-z^2/(2\sigma_{Bz}^2)) \times (1/(2\pi\sigma_{Br}^2)) \cdot \exp(-r^2/(2\sigma_{Br}^2))$ - charge density of a bunch (LAB)
- $\omega_b = 2\pi/\sigma_{Bt} = 1.3 \cdot 10^{13}$ s⁻¹ - typical frequency associated with the bunch length. We will show later that this is indeed the characteristic frequency of the process.
- $\omega_o = 2\pi \cdot \mathcal{F}$ - bunch repetition frequency
- $T = \mathcal{F}^{-1}$ - repetition period

The values of used constants:

- $\varepsilon_o = 8.854 \cdot 10^{-12}$ F/m
- $\mu_o = 4\pi \cdot 10^{-7}$ N/A²
- $k = 6.82 \cdot 10^{-5}$ eV/K - Boltzmann constant

3 Beam Electromagnetic Field

3.1 Calculation of the Electromagnetic Field

The bunch creates an electromagnetic pulse in the pipe. The fields are calculated in two steps: at first, the electric field created by the bunch charge is calculated in the rest frame of the bunch, then the field is boosted to the Lab frame. The variables in the bunch rest frame are marked with prime sign. In this frame, only the radial component of the field matters.

Let us assume that the bunch moves along the z axis in the Lab frame and crosses $z = 0$ at $t = 0$. The bunch rest frame has the same orientation as the Lab frame and its center is at the center of the bunch. We are mostly interested in the field close to the beam, the accuracy at the peripheral area of the pipe is not very important. The bunch size (RMS) in the bunch rest frame is γ times larger than in the Lab frame, namely 25-150 cm at beam energies of 0.85-5.0 GeV, which is much larger than the cell radius of 2 cm. In the limit $r \ll \sigma_{Bz}\gamma$ the flux through a cylinder of the radius r is:

$$\varepsilon_0 E'_r(z', r) \cdot 2\pi r = \int_0^r d\xi \cdot 2\pi\xi \cdot \rho'(z', \xi) = \rho'(z') \cdot (1 - \exp(-\frac{r^2}{2\sigma_{Br}^2})) \quad (1)$$

where

$$\rho'(z') = \frac{q}{\sqrt{2\pi}\sigma_{Bz}\gamma} \cdot e^{-\frac{z'^2}{2(\sigma_{Bz}\gamma)^2}} \quad (2)$$

is the longitudinal charge density along the bunch. The radial component of the electric field is:

$$E'_r(z', r) = \frac{q}{2\pi\varepsilon_0} \frac{1}{\sqrt{2\pi}\sigma_{Bz}\gamma} \cdot \exp(-\frac{z'^2}{2(\sigma_{Bz}\gamma)^2}) (1 - \exp(-\frac{r^2}{2\sigma_{Br}^2})) \frac{1}{r} \quad (3)$$

Now, let us boost the field into the Lab frame using the Lorentz formula:

$$E_r(z, t) = \gamma(E'_r(z') - \vec{V} \times \vec{B}'(z')) \quad (4)$$

$$B_r(z, t) = \gamma(B'_r(z') + \vec{V} \times \vec{E}'(z')/c^2) \quad (5)$$

$$z' = \gamma(z - V \cdot t) \quad (6)$$

where $\vec{V} \sim (0, 0, c)$ is the bunch velocity (along z in our case).

We calculate the radial electric field and the tangential (along ϕ) magnetic field. Indeed, $\vec{V} \times \vec{E}'(z', r) = V \cdot E'_r$ is directed along $\vec{d}\phi$.

$$\begin{aligned} E_r(z, r, t) &= \frac{q\gamma}{2\pi\varepsilon_0} \frac{1}{\sqrt{2\pi}\sigma_{Bz}\gamma} \cdot \exp(-\frac{(z - Vt)^2\gamma^2}{2(\sigma_{Bz}\gamma)^2}) (1 - \exp(-\frac{r^2}{2\sigma_{Br}^2})) \frac{1}{r} = \\ &= \frac{q}{2\pi\varepsilon_0} \frac{1}{\sqrt{2\pi}\sigma_{Bz}} \cdot \exp(-\frac{(z - Vt)^2}{2\sigma_{Bz}^2}) (1 - \exp(-\frac{r^2}{2\sigma_{Br}^2})) \frac{1}{r} \end{aligned} \quad (7)$$

The field profile repeats the bunch profile. The field is γ times larger than in the rest frame and is located in a thin disk around the bunch. In the same way

$$B_T(z, r, t) = \frac{q}{2\pi\varepsilon_0 c} \frac{1}{\sqrt{2\pi}\sigma_{Bz}} \cdot \exp(-\frac{(z - Vt)^2}{2\sigma_{Bz}^2}) (1 - \exp(-\frac{r^2}{2\sigma_{Br}^2})) \frac{1}{r} = E_r(z, r, t)/c \quad (8)$$

For the conditions used the fields in the pulse reach their maximum at $r = 160 \mu\text{m}$, namely $E_r(0, r, 0) = 4.31 \cdot 10^4 \text{ V/m}$ and $B_r(0, r, 0) = 1.44 \cdot 10^{-4} \text{ T}$, while at $r=2 \text{ cm}$ the fields are 478 V/m and $1.59 \cdot 10^{-6} \text{ T}$.

Let us re-write Eq.8:

$$B_T(z, r, t) = B_T(r) \cdot \exp\left(-\frac{(z - Vt)^2}{2\sigma_{Bz}^2}\right) \quad (9)$$

The energy of the field flows along the beam $S = \text{Re}(EH^*)/2 = |B|^2 c/\mu_0/2$ The density of the energy flux of the electromagnetic field of a bunch, passing through the pipe cross-section is:

$$\begin{aligned} \frac{w(r)}{dS} &= \frac{c}{2\mu_0} B_T(r)^2 \cdot \int_{-\infty}^{\infty} dt \exp\left(-\frac{2(ct)^2}{2\sigma_{Bz}^2}\right) = \frac{1}{2\mu_0} B_T(r)^2 \cdot \sqrt{\pi} \sigma_{Bz} = \\ &= \frac{1}{2\mu_0} \left(\frac{q}{2\pi\epsilon_0 c}\right)^2 \frac{1}{\sqrt{4\pi\sigma_{Bz}}} \cdot (1 - \exp(-\frac{r^2}{2\sigma_{Br}^2}))^2 \frac{1}{r^2} \end{aligned} \quad (10)$$

In order to integrate the power flux over the pipe cross section let us make an approximation for $R > 5\sigma_{Br}$:

$$\int_0^R dr \cdot 2\pi r \frac{(1 - e^{-\frac{r^2}{2\sigma_{Br}^2}})^2}{r^2} = 2\pi \int_0^{R/\sigma_{Br}} d\xi \frac{(1 - \exp(-\xi^2/2))^2}{\xi} \approx 2\pi \cdot (1.205 + \ln \frac{R}{5\sigma_{Br}}) \quad (11)$$

The full power of radiation coming down the pipe is determined using the repetition rate \mathcal{F} :

$$W = \mathcal{F} \int_0^{r_0} dr \cdot 2\pi r \cdot \frac{w(r)}{dS} \approx \frac{\mathcal{F}}{2\mu_0} \left(\frac{q}{\epsilon_0 c}\right)^2 \frac{1}{2\pi\sqrt{4\pi\sigma_{Bz}}} (1.205 + \ln \frac{r_0}{5\sigma_{Br}}) \approx 2 \text{ mW} \quad (12)$$

3.2 Electromagnetic Radiation from Beam Pipe Irregularities

Additionally to the radiation coming with each beam bunch there is a radiation, detached from beam, generated on beam pipe irregularities, like pipe diameter changes. The beam loses energy due to this radiation, in contrast with the radiation described in Sec.3.1. The radiation is minimized if the beam pipe has the same diameter everywhere. In our case, beyond the ends of the cell pipe there must be a break to a larger vacuum chamber in order to provide the thermal insulation needed. This break acts like a cavity. Let us approximate this cavity with a regular cavity used in the beam lines at CEBAF. A typical voltage generated on this cavity by the beam bunch of a given charge is $\eta \sim 10 \text{ V/pc}$. From this, we can estimate the full power lost by the beam to radiation:

$$W_c = \eta \cdot \mathcal{I}_b^2 / \mathcal{F} \approx 0.2 \text{ mW} \quad (13)$$

Only a small fraction of this radiation enters the downstream beam pipe, most of it would escape the beam area transversally, since the vacuum chamber is wide in this area.

Therefore, inside the trap pipe, the radiation from pipe irregularities is at least 10-100 times weaker than the radiation created by the passing beam and we neglect it.

3.3 Spectral Density of the Electromagnetic Field

In order to estimate the impact of the electromagnetic radiation we have to calculate its spectral density. At a given point ($z = 0$ for example) the field has a form of Eq.9:

$$f(t) = f_o \cdot \exp\left(-\frac{t^2}{2\tau^2}\right), \quad (14)$$

where f_o is a function of the radius r . Here we use a shorter symbol τ for the RMS of the bunch duration $\tau = \sigma_{Bt}$. First, let us calculate the Fourier transform of one single bunch:

$$f(t) = \frac{1}{\sqrt{2\pi}} \int_{-\infty}^{\infty} d\omega \cdot \hat{f}(\omega) e^{i\omega t}, \quad (15)$$

where

$$\hat{f}(\omega) = \frac{1}{\sqrt{2\pi}} \int_{-\infty}^{\infty} dt \cdot f(t) e^{-i\omega t} = f_o \cdot \tau \cdot \exp\left(-\frac{\omega^2 \tau^2}{2}\right) \quad (16)$$

The spectrum starts dropping at frequencies $\nu = \frac{\omega}{2\pi} \sim \frac{1}{\tau} = 320$ GHz.

The bunches arrive with a period T . The appropriate Fourier series is:

$$f(t) = \sum_{n=-\infty}^{\infty} \hat{f}_n \cdot e^{i\omega_o n t}, \quad (17)$$

where $\omega_o = 2\pi/T$ and

$$\hat{f}_n = \frac{1}{T} \int_{-T/2}^{T/2} dt \cdot f(t) e^{-i\omega t} \approx \frac{1}{T} \int_{-\infty}^{\infty} dt \cdot f(t) e^{-i\omega t} = f_o \sqrt{2\pi} \cdot \frac{\tau}{T} \cdot \exp\left(-\frac{\omega_o^2 n^2 \tau^2}{2}\right), \quad (18)$$

The integral can be taken in the infinite limits since the width of the bunch is much smaller than the period: $\tau \ll T$.

3.4 Depolarization Caused by the Beam RF radiation

The magnetic field B_S splits the ground states of hydrogen into four states with different energies, their properties are summarized in Tab.1.

The dominant transitions caused by an external electromagnetic wave are those with either electron or proton spin flip. The magnetic field of the wave has to be perpendicular to z to cause a flip, since, say $\langle -|\hat{\sigma}_x|+ \rangle = 1$. Indeed, the magnetic field created by the beam is circular and always perpendicular to z . The operator describing the interaction includes both the electron and the proton contributions $\mu_e \hat{\sigma}_x^e + \mu_p \hat{\sigma}_x^p$, but the proton contribution is relatively much smaller and we neglect it. Then, we are left with two transitions, which at $B_S = 8$ T happen at frequencies:

$$|a\rangle \rightarrow |d\rangle \Rightarrow \nu_{ad} = 224.92 \text{ GHz} \quad (19)$$

$$|b\rangle \rightarrow |c\rangle \Rightarrow \nu_{bc} = 223.50 \text{ GHz} \quad (20)$$

The probability of a transition, say $|a\rangle \rightarrow |d\rangle$, caused by a harmonic perturbation $\mu_e \cdot B \cdot e^{i\omega t}$, per the time unit is:

$$\frac{dV_{a \rightarrow d}}{dt} = \frac{2\pi}{\hbar} |\langle d | \mu_e \cdot B \cdot \hat{\sigma}_x^e | a \rangle|^2 \delta(\hbar\omega - (E_d - E_a)) \quad (21)$$

name	wave function	relative energy E	E/k, in K, at $B_S = 8$ T
$ a\rangle$	$\alpha +-\rangle - \beta -+\rangle$	$\mathcal{H}(-1 - 2\sqrt{1 + (\frac{\mu_- B_S}{2\mathcal{H}})^2})$	-5.400
$ b\rangle$	$ - -\rangle$	$\mathcal{H} + \mu_+ B_S$	-5.360
$ c\rangle$	$\alpha - +\rangle + \beta + -\rangle$	$\mathcal{H}(-1 + 2\sqrt{1 + (\frac{\mu_- B_S}{2\mathcal{H}})^2})$	5.366
$ d\rangle$	$ + +\rangle$	$\mathcal{H} - \mu_+ B_S$	5.394

Table 1: Levels of hydrogen in a magnetic field directed along z . The symbol $|+-\rangle$ denotes the state with $m_Z = -1/2$ for the electron and $m_Z = +1/2$ for the proton. The constant $\mathcal{H} = 5.87 \cdot 10^{-6}$ eV defines the hyperfine splitting, namely $4\mathcal{H}/h = 1.420$ GHz, while $\mu_+ = \mu_e + \mu_p$ and $\mu_- = \mu_e - \mu_p$. The factors α and β can be presented as $\alpha = \sin \theta$, $\beta = \cos \theta$, where the mixing angle $\tan 2\theta \approx 0.05/B_S(T)$. At $B_S = 8$ T the admixture of the “wrong” polarization is $\alpha \approx 0.3\%$ in the amplitude and $\sim 10^{-5}$ in the sample.

We neglect the small mixing in the state $|a\rangle$ ($\alpha \rightarrow 0$) and obtain:

$$\frac{dV_{a \rightarrow d}}{dt} = \frac{2\pi}{\hbar^2} |\mu_e \cdot B|^2 \delta(\omega - \omega_{ad}) \quad (22)$$

Let us first calculate the probability that a single bunch causes the transition, using the Fourier transform as in Eq.16:

$$\hat{B} = B_o(r) \cdot \tau \cdot \exp(-\frac{\omega^2 \tau^2}{2}) \quad (23)$$

$$V_{a \rightarrow d}^B = \frac{2\pi}{\hbar^2} \int_{-\infty}^{\infty} d\omega |\mu_e \cdot \hat{B}|^2 \delta(\omega - \omega_{ad}) = 2\pi \left(\frac{\tau \mu_e B_o(r)}{\hbar} \right)^2 \cdot \exp(-\omega_{ad}^2 \tau^2) \quad (24)$$

In order to see the dependence of the result on the input parameters more clearly let us define a dimensionless function:

$$G(r) = (1 - \exp(-\frac{r^2}{2\sigma_{Br}^2})) \frac{r_o}{r}; \quad G(r_o) = 1 \quad (25)$$

where r_o is the pipe radius. Using $c^{-2} = \varepsilon_o \mu_o$ we obtain:

$$V_{a \rightarrow d}^B = \left(\frac{\mathcal{I}_b}{\mathcal{F}} \right)^2 \left(\frac{\mu_o \mu_e}{2\pi \hbar r_o} \right)^2 \cdot \exp(-\omega_{ad}^2 \tau^2) G^2(r) \quad (26)$$

At $r = r_o = 2$ cm $V_{a \rightarrow d}^B = 1.8 \cdot 10^{-14}$, while at the point of the highest field $r = 160$ μm $V_{a \rightarrow d}^B = 1.5 \cdot 10^{-10}$. One bunch does not change the gas polarization in any noticeable way.

If the beam bunches were arriving at random, we could obtain the transition probability per second by multiplying the result of Eq.26 by the repetition rate \mathcal{F} :

$$\frac{dV_{a \rightarrow d}}{dt} = \frac{\mathcal{I}_b^2}{\mathcal{F}} \left(\frac{\mu_o \mu_e}{2\pi \hbar r_o} \right)^2 \cdot \exp(-\omega_{ad}^2 \tau^2) G^2(r) \quad (27)$$

which, at $r = 160$ μm , is $V_{a \rightarrow d} = 7.5\%$ s^{-1} and at $r = r_o$ is $0.9 \cdot 10^{-5}$ s^{-1} . The fraction of the atoms in the cell, converted per second at a given radius is shown on Fig.1 The full conversion rate inside a cylinder of radius R is:

$$\frac{dV_{a \rightarrow d}}{dt}(r < R) = \frac{1}{\pi R^2} \int_0^R dr \cdot 2\pi r \cdot \frac{dV_{a \rightarrow d}}{dt} \quad (28)$$

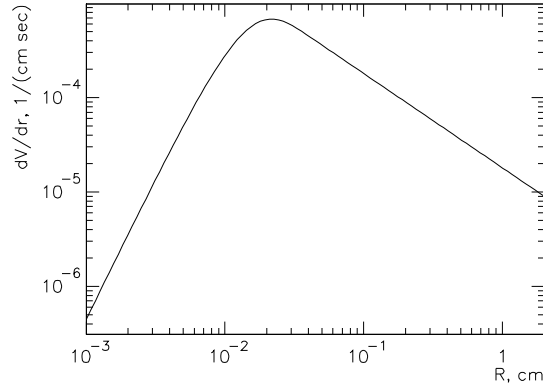


Figure 1: The fraction of the atoms in the cell, converted per second at a given radius $\frac{2\pi r}{\pi r_o^2} \frac{dV_{a \rightarrow d}}{dt}$. Most of the transitions happen at $r \approx 200 \mu\text{m}$.

In the same way as for Eq.11, for $R > 5\sigma_{Br}$:

$$\frac{dV_{a \rightarrow d}}{dt}(r < R) \approx \frac{\mathcal{I}_b^2}{\mathcal{F}} \left(\frac{\mu_o \mu_e}{2\pi \hbar r_o} \right)^2 \cdot \exp(-\omega_{ad}^2 \tau^2) \cdot \frac{2r_o^2}{R^2} \cdot (1.205 + \ln \frac{R}{5\sigma_{Br}}) \quad (29)$$

The conversion rate in a small cylinder $r = 5\sigma_{Br} = 0.5 \text{ mm}$ around the beam is $3.6\% \text{ s}^{-1}$, while in the full cell of $r = r_o = 2 \text{ cm}$ the rate is $0.9 \cdot 10^{-4} \text{ s}^{-1}$. The function Eq.28 reaches its maximum of $6.0\% \text{ s}^{-1}$ at $R = 2.2\sigma_{Br} = 220 \mu\text{m}$.

Let us take into account that the bunches appear at a given frequency, using the Fourier series expansion of Eq.17-18. In the case of a single pulse discussed above, we did not need to consider the spectral density of the gas sample $\frac{dP}{d\omega_{ad}}$. In fact, because of non-uniformity of the magnetic field B_S in the volume of the trap there must be a considerable spread of ω_{ad} in the gas sample. $\frac{dP}{d\omega_{ad}}$ must be peaked at the maximum field in the solenoid and have a tail to lower frequencies. On the other hand, the radiation power is proportional to $\exp(-\omega_{ad}^2 \tau^2)$, which is about 0.6 at 8 T and changes little toward lower fields. Therefore the gas spread over ω_{ad} was neglected in Eq.24.

The probability of a transition per second can be expressed as:

$$\frac{dV_{a \rightarrow d}}{dt} = \frac{2\pi}{\hbar^2} \sum_{n=-\infty}^{\infty} \hat{f}_n \int_{-\infty}^{\infty} d\omega_{ad} \frac{dP}{d\omega_{ad}} \delta(\omega_{ad} - \omega_o n) \quad (30)$$

Let us assume for the moment that the gas density function is narrow enough, that only one peak at $\omega_o k$ happens to be in the region where the density is non-zero. Then:

$$\frac{dV_{a \rightarrow d}}{dt} = \frac{dP}{d\omega_{ad}} \Big|_{\omega_o k} 2\pi \mathcal{I}_b^2 \left(\frac{\mu_o \mu_e}{2\pi \hbar r_o} \right)^2 \cdot \exp(-\omega_o^2 k^2 \tau^2) G^2(r) \quad (31)$$

In order to check this formula let us assume that the gas is distributed evenly on a frequency range of $1/T = \mathcal{F}$. Then, $\frac{dP}{d\omega_{ad}} = 1/2\pi\mathcal{F}$ and Eq.31 becomes equivalent to Eq.27, as it should.

In reality, the gas spectral distribution is much broader and overlaps with a multitude of $\omega_o n$ peaks, as shown on Fig.2, obtained by simulation of a trap in the field of a simple solenoid. Adding all the peaks together would provide a result, similar to the continuous case of Eq.27.

In [1] an RF absorption spectrum for a hydrogen trap at 5 T was presented. The shape of the spectrum is comparable to the simulated one on Fig.2.

One should be able, by adjusting the magnetic field, tune the cell in a way that the beam resonances stay beyond the peaks in the gas spectral density in order to reduce the transitions. This may help if the solenoid has a much more uniform field, in particular at the axis around the beam. Then, more atoms on the beam path stay beyond the RF grid. One may consider making a solenoid 40 cm long with a 10^{-4} uniformity along the central part, 16 cm long. It would require about 10% higher current density at the solenoid edges, than at the center. The simulated spectra are shown on Fig.3. Additionally it should be pointed out that the spectrometer acceptance may cut out the target edges, reducing the contamination further down.

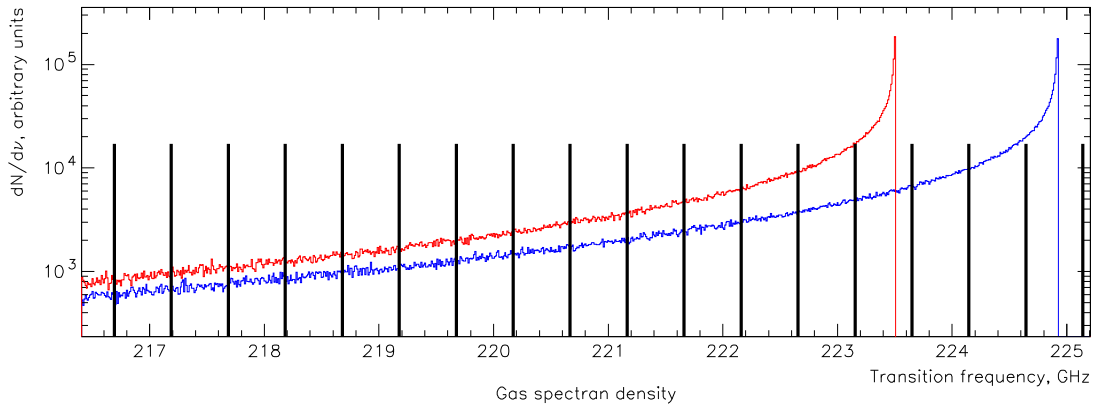


Figure 2: Simulated spectra of the transitions on the axis of the hydrogen trap at 8.0 T, assuming a simple thin solenoid with a constant current density. The density of atoms depends on the field as $\exp(-\mu_e B/kT)$. The transitions $|a\rangle \rightarrow |d\rangle$ and $|a\rangle \rightarrow |c\rangle$, along with the beam frequency grid are shown.

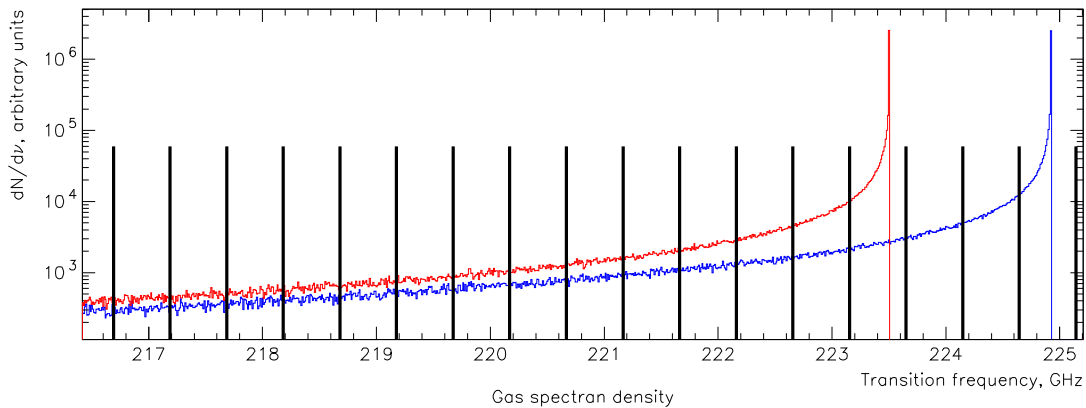


Figure 3: Simulated spectra of the transitions on the axis of the hydrogen trap at 8.0 T, assuming a solenoid with a 10^{-4} field uniformity along the axis.

4 Depolarization of the Target

4.1 RF Generated Depolarization

Let us assume that no considerable reduction of the depolarization rate can be achieved with respect to the estimates from Eq.29 and consider whether it would be acceptable or not for the polarimetry project. The depolarization described have the following features:

- the average rate of conversion is about 10^{-4} of the target density per second;
- at the center around the beam the conversion is about 6% of the density per second.

The “wrong” atoms may disappear by different mechanisms:

- escape the cell by diffusion;
- recombine to a H_2 molecule in gas;
- recombine to a H_2 molecule on the helium coated cell surface.

Here, a crude estimate for the gas diffusion in the target is presented in order to estimate the density of the contamination in the beam area.

Using the atomic interaction cross-section σ , or, parameterizing the atoms by hard spheres of the diameter d , that $\sigma = \pi d^2$, one can calculate the number of atomic collisions one atom takes per second [4]:

$$\frac{dn_{col}}{dt} = \sigma \cdot 4 \frac{dN}{dV} \sqrt{\frac{kT}{\pi m}} = 4d^2 \cdot \frac{dN}{dV} \sqrt{\pi \frac{kT}{m}}, \quad (32)$$

where $\frac{dN}{dV}$ is the gas density and m is the atomic mass. The mean free path in a certain direction, say z , is:

$$\ell_z = \sqrt{v_z^2} / \frac{dn_{col}}{dt} = (4d^2 \frac{dN}{dV} \sqrt{\pi})^{-1}, \quad (33)$$

with $\overline{v_z^2} = kT/m$. There are several calculations of the hydrogen atoms cross-sections [7–11]. One should point out that in the bulk of the polarized hydrogen all the atomic collisions happen in the triplet state of electron spins, while the converted atoms in this gas would interact also in the singlet state. The interaction cross-sections in these two states must be different, since the triplet interaction potential is purely repulsive, while the singlet one is partially attractive [6]. A

Ref., date	conditions	H polarized		H unpolarized	
		$\sigma, 10^{-16} \text{ cm}^2$	$d, 10^{-8} \text{ cm}$	$\sigma, 10^{-16} \text{ cm}^2$	$d, 10^{-8} \text{ cm}$
[8], 1971	T>1 K	87.0	5.26	68.0	4.65
[9], 1977	T~0 K	42.3	3.69	-	-
[10], 1980	T~0 K	6.5	1.44	4.9	1.25
[11], 1983	T=2.5 K	~30.0	3.10	-	-

Table 2: Cross-sections of atomic interactions in polarized and unpolarized atomic hydrogen gas.

large spread of the results (see Tab.2) requires a further investigation of the subject. For these

studies we accepted the value $\sigma = 42.3 \cdot 10^{-16} \text{ cm}^2$, or $d = 3.69 \cdot 10^{-8} \text{ cm}$. This would provide $\frac{dn_{col}}{dt} \approx 1.4 \cdot 10^5 \text{ sec}^{-1}$ and $\ell_z = 0.34 \text{ mm}$ at 300 mK and density of $3 \cdot 10^{15} \text{ cm}^{-3}$.

If the only cleaning mechanism were the diffusion along the pipe toward the end of the trap, we would be able to estimate the average radial profile of the contamination density. Simulation showed that for a pipe with the ratio of length to diameter of 4 the average density created by a “wrong” atom practically does not depend on its point of origin, in other words the transverse diffusion is much faster than the longitudinal one. Simulation also showed that these atoms would drift away from the cell with a time constant of $\approx 1.5 \text{ sec}$ for $d = 0.37 \text{ nm}$ - the triplet interactions. If the full conversion rate in the cell is $10^{-4}/\text{sec}$, the average contamination density in the beam area would be $1.5 \cdot 10^{-4}$ of the normal gas density. This value is proportional to the cross-section of the collisions of the considered atoms.

The conclusion is that the RF-induced transitions should not affect the effective target polarization significantly, providing that the magnetic field is tuned to avoid the resonances. A solenoid with a field uniformity of better than $1 - 4 \cdot 10^{-4}$ on about 40% of its length would help reducing the transition rate.

4.2 Effects Caused by Beam Ionization

In gaseous hydrogen a beam particle releases on average $6.3 \text{ MeV}/(\text{g}/\text{cm}^2)$ by ionization. In the target considered, of the thickness $\sim 3 \cdot 10^{16} \text{ atoms}/\text{cm}^2$, the average loss is 0.3 eV per one beam particle. A part of this energy goes to δ -electrons which may leave the cell spiraling in the magnetic field if their energy is large enough. A reasonable cut-off for the δ -electron kinetic energy is $T_1 \sim 1 \text{ keV}$. At this energy the electron would lose about 100 eV in the target due to ionization losses and carry away the rest of its energy. For the maximum energy we selected $T_2 \sim 0.2T_{max} = 0.2E_{beam}$. Then, the full energy carried away by δ -electrons knocked out by one beam particle would be [5]:

$$E = 0.15 \text{ MeV}/(\text{g}/\text{cm}^2) \cdot \ln \frac{T_2}{T_1} \approx 1.8 \text{ MeV}/(\text{g}/\text{cm}^2) \quad (34)$$

The energy absorbed in the target is $\alpha = 4.5 \text{ MeV}/(\text{g}/\text{cm}^2)$ from one beam particle. The full energy absorbed per unit length of the target per second is:

$$J = \alpha \cdot \frac{\mathcal{I}_b}{q_e} \frac{dN}{N_A dV}, \quad (35)$$

where N_A is the Avogadro number and $\frac{dN}{dV}$ is the gas density.

The heat conductance in gas is [3]:

$$\chi = k \cdot c \frac{dN}{dV} \ell \bar{v}. \quad (36)$$

where $c = 1$ is the specific heat of the atom, ℓ and \bar{v} are the mean free path and average velocity in a given direction. Using Eq.33 we obtain the heat conductance:

$$\chi = \frac{k}{4\sigma} \cdot \sqrt{\pi \frac{kT}{m}}, \quad (37)$$

dependent on the atomic cross-section σ and not dependent on the gas density. Let us assume that the beam profile is flat within a radius r_b , which is an approximation in case the beam is not smeared off by a fast raster and is a good model in the presence of a fast raster. Then, solving the heat flow equation for a very long tube, assuming the fixed temperature T_0 on the tube wall at r_o , we obtain:

$$\begin{aligned} \Delta T(r) = T(r) - T_0 &= \frac{J}{2\pi\chi} \ln \frac{r_o}{r} & r > r_b \\ \Delta T(r) = T(r) - T_0 &= \frac{J}{2\pi\chi} \left[\ln \frac{r_o}{r_b} + \frac{1}{2} \left(1 - \frac{r^2}{r_b^2} \right) \right] & r < r_b \end{aligned} \quad (38)$$

The temperature increase reaches the maximum at the beam center:

$$\Delta T(r) = \alpha \cdot \frac{\mathcal{I}_b}{q_e} \frac{dN}{N_A dV} \frac{2\sigma}{k\pi\sqrt{\pi\frac{kT}{m}}} \left[\ln \frac{r_o}{r_b} + \frac{1}{2} \right] \quad (39)$$

and is proportional to the gas density. For $\mathcal{I}_b = 100 \mu\text{A}$, $\frac{dN}{dV} = 3 \cdot 10^{15} \text{ cm}^{-3}$, $\sigma = \pi d^2$, where $d = 3.7 \cdot 10^{-8} \text{ cm}$, and $T = 0.3 \text{ K}$ we get:

$$\Delta T(0) = 0.051 \text{ K} \cdot \left[\ln \frac{r_o}{r_b} + \frac{1}{2} \right] \quad (40)$$

With no raster ($r_b \approx 200 \mu\text{m}$) $\Delta T(0) = 0.26 \text{ K}$. A raster of $r_b = 2 \text{ mm}$ would decrease it by a factor of ~ 2 : $\Delta T(0) = 0.14 \text{ K}$. Let us evaluate the implications of a temperature rise of 0.14 K . The mean polarization should be not affected in a noticeable way, since the population of oppositely polarized states in the equilibrium would go from $\sim 10^{-16}$ to $\sim 10^{-11}$. However, the density of the target may change considerably. In the state of equilibrium the density depends on temperature as $\exp(-\mu_e B/kT)$, so it may drop by a factor of 300. The situation is more complex, since the temperature is high on the axis and low close to the pipe, so one may expect the warmer gas at the center to bulge out in the magnetic field gradient, diffuse laterally, cool down and return into the cell. But also, one should keep in mind that the energy absorption by the beam is proportional to the gas density. Therefore a dynamic equilibrium should be reached at a certain density. A simplified estimate of this effect gave us the stabilized density of about 20% of the original one, or $\sim 0.6 \cdot 10^{15} \text{ cm}^{-3}$. This, at $100 \mu\text{A}$, would provide an acceptable luminosity. A lower current, as $30 \mu\text{A}$, would stabilize the cell at density of $\sim 1.2 \cdot 10^{15} \text{ cm}^{-3}$. These estimates were done for the atomic cross-section of $\sigma = 42.3 \cdot 10^{-16} \text{ cm}^2$ (see Tab.2), which is in the middle of the range of predictions for this value. The largest value quoted in this table is $\sigma = 87 \cdot 10^{-16} \text{ cm}^2$. For this cross-section, at $30 \mu\text{A}$, the density should stabilize at $\sim 0.75 \cdot 10^{15} \text{ cm}^{-3}$, or 25% of the reference value.

The conclusion is that the heating by beam ionization losses makes a serious impact on the gas storage cell. Simplified calculations show that the target should be still usable, but at a luminosity of about half of the expected. A more thorough modeling of the gas behavior is needed, as well as a thorough comparison of the theoretical calculations, because of the large difference of the predicted atomic cross-sections.

5 Eddy Currents

A bunch moving inside of the conductive pipe induces an electric charge image on the pipe, which moves along the pipe with the bunch, creating “eddy currents”. These currents flow in a thin “skin” of the pipe, the skin depth depends on the characteristic frequency of the electromagnetic pulse. The length of the electromagnetic pulse, created by a point-like moving charge at a distance $r = 0.02$ m from the beam axis is about $r/\gamma \sim 2 \mu\text{m} \ll \sigma_{Bz} = 150 \mu\text{m}$ - the bunch length. Therefore the pulse shape repeats the bunch shape and we may use ω_b for the characteristic frequency.

5.1 Skin Depth and Power Absorption

The skin depth δ estimate is crucial for the power loss calculation. The effect depends, along with already defined frequency ω and conductance σ , on several important parameters:

- τ - mean collision time of electrons in the material
- ℓ - mean free path of electrons in the material
- $\omega_p = \sqrt{\frac{N \cdot q_e^2}{\epsilon_0 m_e}} \approx 1.6 \cdot 10^{16} \text{ s}^{-1}$ - the plasma frequency, where N is the electron density and q_e, m_e are the electron charge and mass.

At frequencies $\omega \ll \omega_p$ three different physics regimes occur, depending on the relative values of these parameters:

- (1) Normal skin effect - low frequency regime: $\omega\tau \ll 1$ and $\ell \ll \delta$. The smallest spacial parameter is the mean free path ℓ . So, on the length of the mean free path the field does not change much. In this case a local (the same space and time) relation $\vec{j} = \sigma \vec{E}$ is valid.
- (2) Anomalous skin effect - a thin skin depth: $\delta \ll \ell$ and $\delta \ll \ell/\omega\tau$, while there is no limit for $\omega\tau$. The lowest spacial parameter is δ .
- (3) High frequency, or infrared limit - $\omega\tau \gg 1$ and $\ell/(\omega\tau) \ll \delta$. In normal metals at normal temperatures this condition is fulfilled in the infrared range.

In order to calculate the power loss let us consider the Maxwell equations for conductors in empty space, neglecting the term $\frac{\partial \vec{D}}{\partial t}$:

$$\text{rot} \vec{H} = \vec{j}; \quad \text{rot} \vec{E} = -\frac{\partial \vec{B}}{\partial t} \quad (41)$$

$$\text{div} \vec{B} = 0; \quad \text{div} \vec{D} = 0 \quad (42)$$

Assuming no magnetic materials: $\vec{B} = \mu_0 \vec{H}$. Let us consider the simplest low frequency regime (1), which adds an equation:

$$\vec{j} = \sigma \vec{E} \quad (43)$$

Then:

$$\Delta \vec{H} = \mu_0 \sigma \frac{\partial \vec{H}}{\partial t} \quad (44)$$

Assuming a time dependence as $e^{-i\omega t}$ we obtain:

$$\Delta \vec{H} = -i\mu_0 \sigma \omega \vec{H} \quad (45)$$

Let us consider high enough frequencies, that the skin depth is much smaller than the conductor size. On the boundary with metal the tangential components of \vec{H} and \vec{E} are conserved. Let us assume that metal occupies all space at $z > 0$. \vec{H} depends only on time and z . Since $div\vec{H} = 0$ and the field somewhere inside the metal is zero, $H_z = 0$ everywhere. We can rewrite Eq.45 as:

$$\frac{\partial^2 \vec{H}}{\partial z^2} + k^2 \vec{H} = 0, \quad (46)$$

where

$$k = \sqrt{\sigma \mu_0 \omega / 2} (1 + i) \quad (47)$$

Then, considering a solution as $\vec{H}_0 \exp(ikz)$ we obtain

$$\vec{H} = \vec{H}_0 \exp(-z/\delta) \exp(iz/\delta - \omega t) \quad (48)$$

where

$$\delta = \sqrt{\frac{2}{\sigma \omega \mu_0}} = \sqrt{\frac{2 \varepsilon_0 c^2}{\sigma \omega}} \quad (49)$$

is the skin depth in the “low frequency” approximation (1). The electrical field is calculated using Eq.43

$$\vec{E} = \zeta \vec{H} \times \vec{n}, \quad (50)$$

where \vec{n} is a vector normal to the surface and ζ is called impedance:

$$\zeta = \sqrt{\frac{\omega \mu_0}{2\sigma}} (1 - i) = \sqrt{\frac{2 \varepsilon_0 c^2}{\sigma \omega}} (1 - i) \quad (51)$$

Both the \vec{H} and \vec{E} are tangential on the surface and are the same inside and outside of the conductor. The power flux into the conductor is described by Poynting vector averaged over time:

$$S = Re(\vec{E} \vec{H}^*) / 2 = Re(\zeta |H| |H|^*) / 2 = Re(\zeta) |H|^2 / 2 = \sqrt{\frac{\omega \mu_0}{2\sigma}} |H|^2 / 2 = \omega \delta \mu_0 |H|^2 / 4 \quad (52)$$

If we apply the “low frequency” limit to our case we obtain:

$$\delta_{lf} = \sqrt{\frac{2 \varepsilon_0 c^2}{\sigma \omega}} = 1.1 \cdot 10^{-9} \text{ m} \quad (53)$$

Now, let us return to our case. Our characteristic frequency is $\omega_b \ll \omega_p$. The other parameters for copper at 0.3 K were estimated using the known conductance, density and assuming that there is one free electron per atom. This estimate is valid, in fact, in the low frequency limit. We assume that all the electrons are drifting in electrical field with a velocity $v_d = q_e E / m_e \cdot \tau$, depending on the time between collisions τ . The current in the conductor is $j = N q_e v_d$. On the other hand, the current can be expressed using the the conductance: $j = \sigma E$, and

$$\tau = \frac{\sigma m_e}{N q_e^2} \approx 4.2 \cdot 10^{-11} \text{ s} \quad (54)$$

We see that $\omega_0\tau \approx 550 \gg 1$. Therefore the low frequency approximation (1) is not applicable in our case. In order to estimate the mean free path ℓ in this framework we have to know the electric field in the metal. Let us make an upper limit estimate. We will see later that in our case the maximum magnetic field parallel to the metal surface is about $B = 2 \cdot 10^{-6}$ T. In the low frequency approximation the associated electric field inside the metal is $B \cdot c\sqrt{2\varepsilon\omega/\sigma} \approx 0.03$ V/m. Therefore $v_d \approx 20$ m/s and

$$\ell \approx v_d \cdot \tau \sim 10^{-9} \text{ m} \quad (55)$$

Therefore $\ell/(\omega\tau) \sim 10^{-12}$ m seems much smaller than a reasonable skin depth δ and we can use the “infrared” approximation (3) of the skin effect. Indeed, we will prove that $\delta \gg \ell/(\omega\tau)$.

A solution for the “infrared” approximation [3] gives

$$\delta = c/\omega_p = 1.8 \cdot 10^{-8} \text{ m}, \quad (56)$$

not dependent on the frequency. It is about 20 times larger than the “low frequency” estimate of Eq.53. The field inside the metal drops exponentially.

It is pointed out in [3] that Eq.56 is obtained neglecting the electron collisions and therefore no absorption of electromagnetic waves in the metal happens. Indeed, the impedance obtained is purely imaginary:

$$\zeta = -i\omega\delta\mu_0 \quad (57)$$

while the energy absorption is defined by real the part of ζ .

Since it is not clear how good is the assumption for no electron collisions we will try to estimate the losses in a different phenomenological approach. The skin depth can be evaluated using the generalized refractive index of the metal:

$$n = n_R - i \cdot n_I, \quad (58)$$

where n_R and n_I are positive and the latter is responsible for the the wave attenuation. The wave inside the metal is suppressed by a factor $\exp(-\omega z \cdot n_I/c)$ and the skin depth is:

$$\delta = \frac{c}{\omega n_I} \quad (59)$$

There is a general description of the refractive index using a simple model for electron motion in material [12]:

$$n^2 = 1 + \frac{\sigma}{i\varepsilon_0\omega(1 + i\omega\tau)}, \quad (60)$$

where σ is the conductance and τ is the mean time between collisions for the electrons in metal. It is evaluated as:

$$\tau \approx \frac{m \cdot \sigma}{N \cdot q_e}, \quad (61)$$

At low frequencies, such as $\omega\tau \ll 1$, an approximation is valid:

$n^2 \approx -i\sigma/(\varepsilon_0\omega)$, and

$$n = \sqrt{\frac{\sigma}{2\varepsilon_0\omega}}(1 - i) \quad (62)$$

The wave inside the material is suppressed by a factor $\exp(-\omega z \cdot n_I/c)$ and the skin depth is:

$$\delta = \frac{c}{\omega n_I} = \sqrt{\frac{2\varepsilon_0 c^2}{\sigma \omega}} \quad (63)$$

the same as in Eq.53. We calculated the refractive index in the range of

$$2.5 \cdot 10^{10} \text{ s}^{-1} \ll \omega \ll 2 \cdot 10^{16} \text{ s}^{-1} \quad (64)$$

or

$$7.5 \text{ cm} \gg \lambda \gg 100 \text{ nm},$$

relevant for our case.

$$n^2 = -\frac{\sigma}{\varepsilon_0 \omega_b^2 \tau} \left(1 - i \cdot \frac{1}{\omega_b \tau}\right) = A \cdot e^{i\phi_0}, \quad (65)$$

where $A \approx \frac{\sigma}{\varepsilon_0 \omega_b^2 \tau}$ and $\phi_0 \approx \pi + \epsilon + 2\pi m$. In order to keep $n_R > 0$ and $n_I > 0$ we select $m = 1$. So,

$$n = \sqrt{A} e^{i(\frac{3}{2}\pi + \epsilon/2)} \approx \sqrt{\frac{\sigma}{\varepsilon_0 \omega_b^2 \tau}} \left(\frac{1}{2\omega_b \tau} - i\right) \approx 3 - 1500i, \quad (66)$$

the refractive index is nearly purely imaginary and the skin depth

$$\delta = \sqrt{\frac{\varepsilon_0 \tau c^2}{\sigma}} \approx 1.8 \cdot 10^{-8} \text{ m}, \quad (67)$$

does not depend on the frequency and matches very well the result in Eq.56!

In order to estimate the absorption let us use the general wave reflection/refraction formalism. In case of a plane wave propagating in a medium with the refractive index $n = n_1$ normally to a plane boundary of another medium with $n = n_2$ the relative reflected intensity can be expressed as:

$$\frac{I_{refl}}{I_0} = \frac{|n_1 - n_2|^2}{|n_1 + n_2|^2} \quad (68)$$

Assuming that the first medium is vacuum and using Eq.58 for the second one:

$$\frac{I_{refl}}{I_0} = \frac{|(1 - n_R) + i \cdot n_I|^2}{|(1 + n_R) - i \cdot n_I|^2} = \frac{(1 - n_R)^2 + n_I^2}{(1 + n_R)^2 + n_I^2} \quad (69)$$

Using Eq.66 we see that about $5 \cdot 10^{-6}$ of the incident power is not reflected but, presumably, absorbed. For an ideal metal ($\sigma \rightarrow \infty$) n is purely imaginary and 100% of the wave is reflected. In “low frequency” limit about $1 \cdot 10^{-4}$ is not reflected, to be compared with $0.25 \cdot 10^{-4}$ obtained using Eq.52.

5.2 Wave Absorption

Let us assume that the “low frequency” formula Eq.52 is applicable for the energy absorbed in the pipe, but let us use the skin depth as a parameter:

$$S = \frac{\omega \delta}{4\mu_0} |B|^2 \quad (70)$$

The power release in the pipe is calculated in the same way as Eq.10, using $\omega = \omega_b = 2\pi/\sigma_{Bt}$

$$P = \mathcal{F} \cdot 2\pi r_0 L \cdot \int_{-\infty}^{\infty} dt S = \delta \frac{q^2 \mathcal{F} L}{8\sqrt{2}c^2 \varepsilon_0 \sigma_{Bt}^2 r_0} \quad (71)$$

For estimating the upper limit on the power let us use the larger skin depth we obtained in Eq.56 $\delta = 1.8 \cdot 10^{-8} m$:

$$P \approx 3 \cdot 10^{-6} W \quad (72)$$

We should keep in mind that in this approximation the impedance is nearly purely imaginary and the power absorption should be much lower than described by Eq.70. Therefore we can say that in fact

$$P < 3 \cdot 10^{-6} W \quad (73)$$

References

- [1] W.A. Kaufman, T. Roser and B. Vuaridel, Nucl. Instrum. Meth. A **335**, 17 (1993).
- [2] I.F. Silvera and J.T.M. Walraven, “Spin Polarized Atomic Hydrogen”, in *Progress in Low Temperature Physics*, (Elsevier Science Publisher B.V., Amsterdam), Vol. X, 139-370 (1986).
- [3] E. M. Livshitz, L. P. Pitaevski, “Physical Kinetics”, Theoretical Physics, **vol X** Nauka, Moscow, 1979
- [4] L. D. Landau, E. M. Livshitz, “Statistical Physics”, Theoretical Physics, **vol X** Nauka, Moscow, 1979
- [5] K. Hagiwara *et al.* [Particle Data Group Collaboration], Phys. Rev. D **66**, 010001 (2002).
- [6] W. Kolos, L. Wolniewicz, “Variational Calculation Of The Long-Range Interaction Between Two Ground-State Hydrogen Atoms”, Chem. Phys. Lett. **24**, 457 (1974).
- [7] M. E. Gersh and R. B. Bernstein, “Calculated total elastic scattering cross sections for H(IS) at collision energies below 1 eV”, Chem. Phys. Lett. **4**, 221 (1969).
- [8] A. C. Allison and F. J. Smith, “Transport properties of atomic hydrogen”, Atomic Data **3**, 317 (1971).
- [9] M. D. Miller and L. H. Nosanow, “Possible new quantum systems. II. Properties of the isotopes of spin-aligned hydrogen”, Phys. Rev. **B15**, 4376 (1977).
- [10] D. G. Friend and R. D. Eppers, “A dilute hard-sphere Bose-gas model calculation of low-density atomic hydrogen gas properties”, J. Low Temp. Phys. **39**, 409 (1980).
- [11] C. Lhuillier, “Transport properties in a spin polarized gas. III”, Journal de Physique **44**, 1 (1983)

- [12] R. P. Feynman, R. B. Leighton, M. L. Sands, "The Feynman Lectures on Physics," **vol 7**, London, UK : Addison-Wesley/Benjamin, 1964